



Unsteady heat and mass transfer from a rotating vertical cone with a magnetic field and heat generation or absorption effects

Ali J. Chamkha*, Ali Al-Mudhaf

Manufacturing Engineering Department, The Public Authority for Applied Education and Training, P.O. Box 42325, Shuweikh 70654, Kuwait

Received 12 January 2004; received in revised form 14 April 2004; accepted 15 June 2004

Abstract

This work is focused on the study of unsteady heat and mass transfer by mixed convection flow over a vertical permeable cone rotating in an ambient fluid with a time-dependent angular velocity in the presence of a magnetic field and heat generation or absorption effects. The cone surface is maintained at variable temperature and concentration. Fluid suction or injection is assumed to occur at the cone surface. The coupled nonlinear partial differential equations governing the thermosolutal mixed convective flow have been solved numerically using an implicit, iterative finite-difference scheme. Comparisons with previously published work have been conducted and the results are found to be in excellent agreement. A parametric study showing the effects of the buoyancy parameter, suction or injection velocity and heat generation or absorption coefficient on the local tangential and azimuthal skin friction coefficients, and the local Nusselt and Sherwood numbers is conducted. These are illustrated graphically to depict special features of the solutions. It is found that the local tangential and azimuthal skin-friction coefficients and local Nusselt and Sherwood numbers increase with the time when the angular velocity of the cone increases, but the reverse trend is observed for decreasing angular velocity. However, these are not mirror reflection of each other. Increasing the buoyancy ratio is predicted to increase the skin-friction coefficients and the Nusselt and Sherwood numbers. Also, increases in the heat generation or absorption coefficient increase the local tangential skin-friction coefficient and Sherwood number and decrease the local Nusselt number. On the other hand, the azimuthal skin-friction coefficient and the Nusselt and Sherwood numbers increase (decrease) with the increase in the suction (injection) parameter.

© 2004 Elsevier SAS. All rights reserved.

Keywords: Rotating cone; Unsteady flow; MHD; Heat transfer; Mass transfer; Heat generation/absorption; Suction/injection

1. Introduction

The study of flow and (or) heat and mass transfer over rotating bodies is of considerable interest due its occurrence in many industrial, geothermal, geophysical, technological and engineering applications. Such a study is important in the design of turbines and turbo-machines, in estimating the flight path of rotating wheels and spin-stabilized missiles and in the modeling of many geophysical vortices. As explained by Takhar et al. [1], when an axisymmetric body rotates in a forced flow field, the fluid near the surface of the body is forced outward in the radial direction due to the action of

the centrifugal force. This fluid is then replaced by the fluid moving in the axial direction. Thus, the axial velocity of the fluid in the vicinity of a rotating body is more than that of a stationary body. This increase in the axial velocity enhances the convective heat transfer between the body and the fluid. This principle has been used to develop practical systems for increasing heat transfer. For example, the utility of rotating condensers for sea-water distillation and space-craft power plants in a zero-gravity environment was shown by Hickman [2]. Ostrach and Braun [3] have investigated the possibility of cooling the nose-cone of re-entry vehicles by spinning the nose. Also, rotating heat exchangers are extensively used by the chemical and automobile industries. Early investigations of flow and heat transfer in rotating systems are given by Dorffman [4] and Kreith [5].

* Corresponding author. Tel. and fax: +965-483-2761.

E-mail addresses: chamkha@paaet.edu.kw (A.J. Chamkha), ali246@paaet.edu.kw (A. Al-Mudhaf).

Nomenclature

B_0 magnetic induction
 c concentration
 c_p specific heat at constant pressure. $\text{kJ}\cdot\text{kg}^{-1}\cdot\text{K}^{-1}$
 c_{w0} wall concentration at time $t^* = 0$
 C dimensionless concentration,
 $= (c - c_\infty)/(c_w - c_\infty)$
 C_{fx} tangential skin friction coefficient,
 $= -Re_x^{-1/2} \phi(t^*) H''(0, t^*)$
 C_{fy} azimuthal skin friction coefficient,
 $= -2Re_x^{-1/2} \phi(t^*) G'(0, t^*)$
 D mass diffusivity $\dots\dots\dots \text{m}^2\cdot\text{s}^{-1}$
 E electric field
 g gravitational acceleration $\dots\dots\dots \text{m}\cdot\text{s}^{-2}$
 G, H dimensionless similarity velocity functions
 Gr_L Grashof number,
 $= g\beta_T \cos \alpha (T_w - T_\infty) L^3 / \nu^2$
 Ha^2 square of Hartmann number, $= \sigma B_0^2 L^2 / \mu$
 H_0 dimensionless suction or injection velocity,
 $= w_0 / [v(\Omega_0 \sin \alpha)^{1/2}]$
 k fluid thermal conductivity $\dots\dots\dots \text{W}\cdot\text{m}^{-1}\cdot\text{K}^{-1}$
 L characteristic length $\dots\dots\dots \text{m}$
 M magnetic parameter, $= Ha^2 / Re_L$
 N buoyancy ratio, $= \beta_c (c_w - c_\infty) / [\beta_T (T_w - T_\infty)]$
 Nu_x local Nusselt number, $= -Re_x^{1/2} \theta'(0, t^*)$
 Pr Prandtl number, $= \rho \nu c_p / k$
 Q_0 dimensional heat generation or absorption coefficient
 Re_L Reynolds number, $= \Omega_0 L^2 \sin \alpha / \nu$
 Re_m magnetic Reynolds number, $= \mu_0 \sigma V L$
 Re_x local Reynolds number, $= \Omega_0 x^2 \sin \alpha / \nu$
 Sc Schmidt number, $= \nu / D$
 Sh_x local Sherwood number, $= -Re_x^{1/2} C'(0, t^*)$
 t dimensional time $\dots\dots\dots \text{s}$
 t^* dimensionless time, $= (\Omega_0 \sin \alpha) t$
 T temperature $\dots\dots\dots \text{K}$

T_{w0} wall temperature at time $t^* = 0 \dots\dots\dots \text{K}$
 u, v, w velocity components $\dots\dots\dots \text{m}\cdot\text{s}^{-1}$
 V characteristic velocity $\dots\dots\dots \text{m}\cdot\text{s}^{-1}$
 w_0 suction or injection velocity $\dots\dots\dots \text{m}\cdot\text{s}^{-1}$
 x, y, z curvilinear coordinates

Greek symbols

α semi-vertical angle of the cone
 β_c coefficient of concentration expansion
 β_T coefficient of thermal expansion
 Δ dimensionless heat generation or absorption coefficient, $= Q_0 / (\rho c_p \Omega_0 \sin \alpha)$
 ε a constant used in the continuous function of time
 η similarity variable, $= (\Omega_0 \sin \alpha / \nu)^{1/2} z$
 $\phi(t^*)$ continuous function of time
 λ buoyancy parameter (Richardson number),
 $= Gr_L / Re_L^2$
 μ dynamic viscosity $\dots\dots\dots \text{kg}\cdot\text{m}^{-1}\cdot\text{s}^{-1}$
 μ_0 magnetic permeability
 ν kinematic viscosity $\dots\dots\dots \text{m}^2\cdot\text{s}^{-1}$
 ρ fluid density $\dots\dots\dots \text{kg}\cdot\text{m}^{-3}$
 σ electrical conductivity
 θ dimensionless temperature,
 $= (T - T_\infty) / (T_w - T_\infty)$
 Ω angular velocity of the cone $\dots\dots\dots \text{s}^{-1}$
 Ω_0 angular velocity of the cone at $t = 0 \dots\dots \text{s}^{-1}$

Subscripts

i initial condition
 t, x, z partial derivatives with respect to t, x and z , respectively
 w condition at the wall
 ∞ condition at free stream

The problem of forced convection from isothermal and non-isothermal disks rotating in an ambient fluid was investigated by Sparrow and Gregg [6] and Hartnett [7], respectively. Tien and Tsugi [8], and Koh and Price [9] have presented a theoretical analysis of the forced flow and heat transfer past a rotating cone. The influence of the Prandtl number on the heat transfer on rotating non-isothermal disks and cones was investigated by Hartnett and Deland [10]. The effect of the axial magnetic field on the flow and heat transfer over a rotating disk was considered by Sparrow and Cess [11]. Tarek et al. [12] have obtained an asymptotic solution of the flow problem over a rotating disk with a weak axial magnetic field. Lee et al. [13] have studied the flow and heat transfer over a rotating body of revolution (sphere). Wang [14] has investigated the flow and heat transfer on rotating cones, disks and axisymmetric bodies with concentrated

heat sources. The laminar natural convection from a non-isothermal cone was analyzed by Hering and Grosh [15] and Roy [16]. An approximate method of solution for the overall heat transfer from vertical cones in laminar natural convection was reported by Alamgir [17]. The laminar natural convection over a slender vertical frustum of a cone has been studied by Na and Chiou [18,19]. Yih [20] has considered the effects of thermal radiation on natural convection about a truncated cone. The similarity solution of the mixed convection from a rotating vertical cone in an ambient fluid was obtained by Hering and Grosh [21] for Prandtl number $Pr = 0.7$ and by Himasekhar et al. [22] for a wide range of Prandtl numbers. Recently, Anilkumar and Roy [23] have obtained similarity solutions for the problem of unsteady mixed convection from a rotating vertical cone in a rotating fluid in the presence of thermal and mass diffusion.

All of the above studies deal with steady flows. In many practical problems, the flow could be unsteady due to the angular velocity of the spinning body which varies with time or due to the impulsive change in the angular velocity of the body. The unsteady boundary layer flow of an impulsively-started translating and spinning rotational symmetric body has been investigated by Ece [24], who obtained the solution for small time. The corresponding heat transfer problem has been considered by Ozturk and Ece [25]. Takhar et al. [26] have solved the problem of unsteady laminar MHD flow and heat transfer in the stagnation region of an impulsively spinning and translating sphere in the presence of buoyancy forces. More recently, Roy and Anilkumar [27] have considered the problem of unsteady mixed convection from a rotating cone in a rotating fluid due to the combined effects of thermal and mass diffusion for the conditions of prescribed wall temperature and heat flux.

In this paper, the problem of unsteady heat and mass transfer by mixed convective flow over a rotating vertical permeable cone in the presence of a magnetic field and heat generation or absorption effects is considered. This problem represents a generalization of the problems considered earlier by Takhar et al. [1] and Roy and Anilkumar [27] for the case of prescribed wall temperature. The unsteadiness in the flow field is due to the angular velocity of the cone which varies arbitrarily with time. The coupled nonlinear parabolic partial differential equations governing the flow and heat and mass transfer problem have been solved numerically using an implicit iterative finite-difference scheme.

2. Problem formulation

Consider unsteady, laminar, non-dissipative, constant property, incompressible boundary-layer heat and mass transfer by mixed convective axisymmetric flow of an electrically-conducting and heat generating or absorbing fluid over a heated vertical permeable cone rotating in an ambient fluid with time-dependent angular velocity, $\Omega(t^*) = \Omega_0 \phi(t^*)$, $t^* = (\Omega_0 \sin \alpha)t$, around the axis of the cone. Uniform fluid suction or injection with velocity w_0 is assumed to occur at the cone surface. A uniform magnetic field of strength B_0 is applied in the z -direction (normal direction) and the gravitational acceleration g acts downward parallel to the axis of the cone. The physical model and the coordinate system are shown in Fig. 1. The rectangular curvilinear fixed coordinate system (x, y, z) , where x is measured along a meridional section, the y -axis is along a circular section, and the z -axis is normal to the cone surface have been employed. Let u, v and w be the velocity components along the x (tangential), y (circumferential or azimuthal) and z (normal) directions, respectively. The wall temperature T_w and wall concentration c_w are assumed to vary linearly with the distance x and the ambient temperature (T_∞) and concentration (c_∞) are constant. The cone surface is assumed to be electrically-insulated. The magnetic Reynolds number is as-

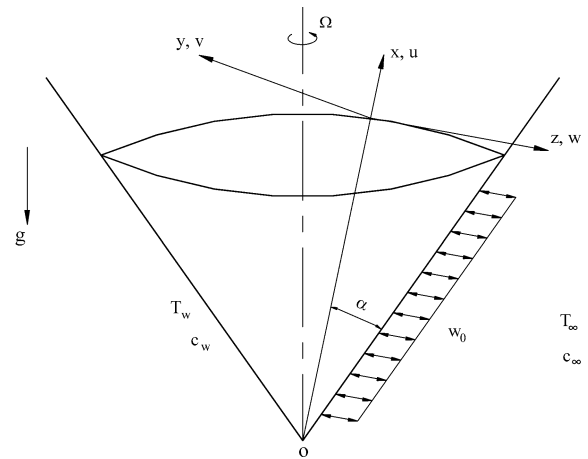


Fig. 1. Physical model and coordinate system.

sumed to be small ($Re_m = \mu_0 \sigma V L \ll 1$ where μ_0 and σ are the magnetic permeability and the electrical conductivity, and V and L are the characteristic velocity and length, respectively). Under this condition, it is possible to neglect the induced magnetic field in comparison to the applied magnetic field. Since there is no applied or polarization voltage imposed on the flow field, the electric field $\vec{E} = 0$. Hence, Maxwells' equations are uncoupled from the Navier–Stokes equations (see Cramer and Pai [28]) and the only contribution of the magnetic field is the Lorentz force in the absence of the Hall effect. Under the above assumptions and using the Boussinesq approximation, the boundary-layer equations governing this heat and mass transfer convective flow on the rotating cone [8,11,22] are given by

$$u_x + x^{-1}u + w_z = 0 \tag{1}$$

$$u_t + uu_x + wu_z - v^2/x = vu_{zz} + g\beta_T \cos \alpha (T - T_\infty) + g\beta_c \cos \alpha (c - c_\infty) - \sigma B_0^2 u / \rho \tag{2}$$

$$v_t + uv_x + wv_z + uv/x = vv_{zz} - \sigma B_0^2 v / \rho \tag{3}$$

$$T_t + uT_x + wT_z = (v/Pr)T_{zz} + Q_0/(\rho c_p)(T - T_\infty) \tag{4}$$

$$c_t + uc_x + wc_z = Dc_{zz} \tag{5}$$

The initial conditions are given by the steady-state equations:

$$\begin{aligned} u(x, z, 0) &= u_i(x, z) \\ v(x, z, 0) &= v_i(x, z), \quad w(x, z, 0) = w_i(x, z) \\ T(x, z, 0) &= T_i(x, z), \quad c(x, z, 0) = c_i(x, z) \end{aligned} \tag{6}$$

The boundary conditions for this problem are given by

$$\begin{aligned} u(x, 0, t) &= 0 \\ w(x, 0, t) &= w_0, \quad v(x, 0, t) = \Omega_0 x \sin \alpha \phi(t^*) \\ T(x, 0, t) &= T_w(x), \quad c(x, 0, t) = c_w(x) \\ u(x, \infty, t) &= v(x, \infty, t) = 0, \quad T(x, \infty, t) = T_\infty \\ c(x, \infty, t) &= c_\infty \end{aligned}$$

$$\begin{aligned} u(\infty, z, t) = v(\infty, z, t) = 0, \quad T(\infty, z, t) = T_\infty \\ c(\infty, z, t) = c_\infty, \quad z > 0 \end{aligned} \quad (7)$$

Here T is the temperature; c is the concentration; β_T is the coefficient of the thermal expansion; β_c is the coefficient of the concentration expansion; α is the semi-vertical angle of the cone; ν is the kinematic viscosity; c_p is the specific heat at constant pressure, ρ is the density of the fluid; t and t^* ($t^* = \Omega_0 t$) are the dimensional and dimensionless times, respectively; Ω_0 is the angular velocity of the cone at $t = 0$; Pr is the Prandtl number; D is the mass diffusivity, Q_0 is the dimensional heat generation or absorption coefficient; $\phi(t^*)$ is a continuous function having continuous first-order derivative; the subscripts t , x and z denote partial derivatives with respect to t , x and z , respectively; the subscript i denotes initial conditions; and the subscripts w and ∞ denote wall and ambient conditions, respectively.

It is convenient to transform Eqs. (1)–(5) into the (η, t^*) system by applying the following transformations;

$$\begin{aligned} \eta &= (\Omega_0 \sin \alpha / \nu)^{1/2} z, \quad t^* = (\Omega_0 \sin \alpha) t \\ u(x, z, t) &= -2^{-1} (\Omega_0 \sin \alpha) H'(\eta, t^*) \phi(t^*) \\ v(x, z, t) &= (\Omega_0 x \sin \alpha) G(\eta, t^*) \phi(t^*) \\ w(x, z, t) &= \nu (\Omega_0 \sin \alpha)^{1/2} H(\eta, t^*) \phi(t^*) \\ T(x, z, t) - T_\infty &= (T_w - T_\infty) \theta(\eta, t^*) \\ T_w - T_\infty &= (T_{w0} - T_\infty) x / L \\ c(x, z, t) - c_\infty &= (c_w - c_\infty) C(\eta, t^*) \\ c_w - c_\infty &= (c_{w0} - c_\infty) x / L \\ Gr_L &= g \beta_T \cos \alpha (T_w - T_\infty) L^3 / \nu^2 \\ Re_L &= \Omega_0 L^2 \sin \alpha / \nu, \quad \lambda = Gr_L / Re_L^2 \\ N &= \beta_c (c_w - c_\infty) / [\beta_T (T_w - T_\infty)] \\ M &= Ha^2 / Re_L, \quad Sc = \nu / D \\ Ha^2 &= \sigma B_0^2 L^2 / \mu, \quad \Delta = Q_0 / (\rho c_p \Omega_0 \sin \alpha) \end{aligned} \quad (8)$$

where T_{w0} and c_{w0} the wall temperature and concentration at time $t^* = 0$, respectively. With these transformations, Eq. (1) is identically satisfied and Eqs. (2)–(5) reduce to the following system of equations,

$$\begin{aligned} H''' - \phi H H'' + 2^{-1} \phi (H')^2 - 2\phi G^2 \\ - 2\phi^{-1} \lambda (\theta + NC) - MH' \\ - \phi^{-1} (d\phi/dt^*) H' - \partial H' / \partial t^* = 0 \end{aligned} \quad (9)$$

$$G'' - \phi (HG' - H'G) - MG - \partial G / \partial t^* = 0 \quad (10)$$

$$\theta'' - Pr(H\theta' - 2^{-1} H'\theta) \phi + Pr\Delta\theta - Pr\partial\theta/\partial t^* = 0 \quad (11)$$

$$C'' - Sc(HC' - 2^{-1} H'C) \phi - Sc\partial C/\partial t^* = 0 \quad (12)$$

The boundary conditions (7) can be rewritten as

$$\begin{aligned} H(0, t^*) = H_0/\phi(t^*), \quad H'(0, t^*) = 0 \\ G(0, t^*) = \theta(0, t^*) = C(0, t^*) = 1 \\ H'(\infty, t^*) = G(\infty, t^*) = \theta(\infty, t^*) = C(\infty, t^*) = 0 \end{aligned} \quad (13)$$

where $H_0 = w_0 / [\nu (\Omega_0 \sin \alpha)^{1/2}]$ is the dimensionless suction or injection velocity. Eqs. (9)–(13) reduce to those of Takhar et al. [1] when Eq. (12) is ignored and $H_0 = N = \Delta = 0$. Also, they reduce to those reported by Roy and Anilkumar [27] for the case of prescribed wall temperature (with $\alpha_1 = 1$) when $H_0 = M = \Delta = 0$.

The initial conditions (i.e., conditions at $t^* = 0$) are given by the steady state equations obtained from (9)–(12) by putting $\phi = 1$, $d\phi/dt^* = \partial H'/\partial t^* = \partial G/\partial t^* = 0$ when $t^* = 0$. The steady-state equations are

$$\begin{aligned} H''' - HH'' + 2^{-1} (H')^2 - 2G^2 \\ - 2\lambda(\theta + NC) - MH' = 0 \end{aligned} \quad (14)$$

$$G'' - (HG' - H'G) - MG = 0 \quad (15)$$

$$\theta'' - Pr(H\theta' - 2^{-1} H'\theta) + Pr\Delta\theta = 0 \quad (16)$$

$$C'' - Sc(HC' - 2^{-1} H'C) = 0 \quad (17)$$

with boundary conditions

$$\begin{aligned} H(0) = H_0, \quad H'(0) = 0, \quad G(0) = \theta(0) = C(0) = 1 \\ H'(\infty) = G'(\infty) = \theta(\infty) = C(\infty) = 0 \end{aligned} \quad (18)$$

Here η and t^* are the transformed coordinates; H' , G and H are the dimensionless velocity components along the tangential, azimuthal and normal directions, respectively; θ is the dimensionless temperature; C is the dimensionless concentration; Gr_L is the Grashof number; Re_L is the Reynolds number; λ is the dimensionless buoyancy parameter; N is the buoyancy ratio such that $N < 0$ corresponds to opposing flow while $N > 0$ corresponds to aiding flow; M is the dimensionless magnetic parameter; Ha^2 is the Hartmann number; Δ is the dimensionless heat generation or absorption coefficient; L is the characteristic length; Sc is the Schmidt number; μ is the coefficient of viscosity; and a prime denotes a derivative with respect to η .

It may be remarked that the steady-state equations (14)–(16) in the absence of all of the magnetic field ($M = 0$), buoyancy ratio ($N = 0$) and heat generation or absorption effects ($\Delta = 0$) are identical to those of Himasekhar et al. [22] if we replace H' by $-2F$ and λ by Gr/Re^2 . Furthermore, Eqs. (14)–(16) in the absence of the buoyancy and heat generation or absorption effects ($\lambda = 0$, $\Delta = 0$) and for constant wall temperature case are the same as those of Sparrow and Cess [11] if the term $Pr H'\theta/2$, which is the contribution due to the linear variation of the wall temperature with the distance x is omitted.

Of special interest for this problem are the local skin friction coefficients in the tangential and azimuthal directions, the local Nusselt number and the local Sherwood number. These physical quantities are respectively given by

$$\begin{aligned} C_{fx} &= 2\mu(\partial u/\partial z)_{z=0} / [\rho(\Omega_0 x \sin \alpha)^2] \\ &= -Re_x^{-1/2} \phi(t^*) H''(0, t^*) \end{aligned}$$

$$\begin{aligned} C_{fy} &= -2\mu(\partial v/\partial z)_{z=0} / [\rho(\Omega_0 x \sin \alpha)^2] \\ &= -2Re_x^{-1/2} \phi(t^*) G'(0, t^*) \end{aligned}$$

$$Nu_x = -x(\partial T/\partial z)_{z=0}/(T_w - T_\infty) = -Re_x^{1/2}\theta'(0, t^*)$$

$$Sh_x = -x(\partial c/\partial z)_{z=0}/(c_w - c_\infty) = -Re_x^{1/2}C'(0, t^*) \quad (19)$$

where $Re_x = \Omega_0 x^2 \sin \alpha / \nu$ is the local Reynolds number.

3. Numerical method

The coupled nonlinear parabolic partial differential equations (9)–(12) under boundary conditions (13) and initial conditions (14)–(18) have been solved numerically using an implicit, iterative tri-diagonal finite-difference scheme similar to that discussed by Blottner [29]. All first-order derivatives with respect to t^* are replaced by two-point backward difference formulae of the form

$$\partial R/\partial t^* = (R_{i,j} - R_{i-1,j})/\Delta t^* \quad (20)$$

where R represents the dependent variables H or G or θ or C and i and j are node locations in the t^* and η directions, respectively. First, the third-order partial differential equation (9) is converted into a second-order partial differential equation by substituting $H' = N$. Then the second-order partial differential equations for N , G , θ and C are discretized using three-point central difference formulae, while first-order derivatives with respect to η are discretized by employing the trapezoidal rule. At each line of constant t^* , a system of algebraic equations is obtained. The nonlinear terms of these equations are evaluated at the previous iteration and the system of algebraic equations is then solved with iteration by using the well-known Thomas algorithm (see Blottner [29]). The same procedure is repeated for the next t^* value and the problem is solved line by line until the desired t^* value is reached. A convergence criterion based on the relative difference between the current and previous iterations is employed. When this difference reaches 10^{-5} , the solution is assumed to have converged and the iteration process is terminated.

4. Results and discussion

In this section, numerical results for the velocity, temperature and concentration profiles as well as the local skin friction coefficients in the tangential and azimuthal directions, the local Nusselt number and the local Sherwood number based on the finite-difference methodology discussed earlier are presented and/or discussed for various values of the physical parameters. The results have been obtained for both increasing and decreasing angular velocities [$\phi(t^*) = 1 + \epsilon t^{*2}$, $\epsilon = \pm 0.2$, $0 \leq t^* \leq 2$] for several values of the buoyancy ratio N ($-0.5 \leq N \leq 5$), the dimensionless suction or injection velocity H_0 ($-3 \leq H_0 \leq 3$), and dimensionless heat generation or absorption coefficient Δ ($-2 \leq \Delta \leq 1.5$). The influence of the other physical parameters involved in the problem were presented earlier by Takhar et al. [1] in the

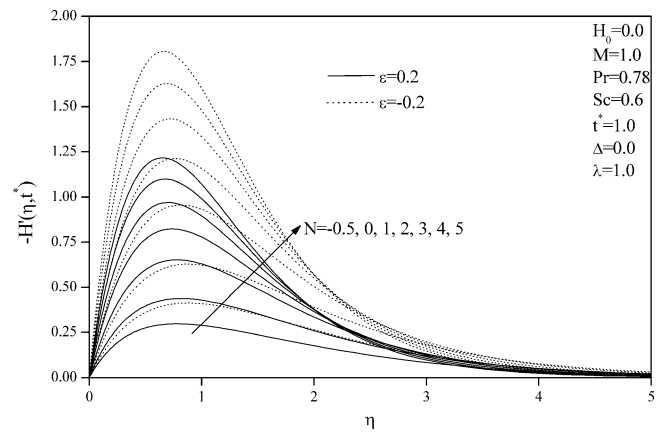


Fig. 2. Effect on N on velocity profiles $-H'(\eta, t^*)$.

absence of mass transfer, surface transpiration and heat generation or absorption effects. For brevity and page limitation, the effect of these parameters (λ , M and Pr) on the solutions will not be repeated herein.

In order to assess the accuracy of the numerical method, the present results were compared with the steady-state results for the surface shear stresses in the tangential and azimuthal directions [$-H''(0)$, $-G'(0)$], and the surface heat transfer [$-\theta'(0)$] in the absence of the magnetic field ($M = 0$), mass transfer ($N = 0$), surface transpiration ($H_0 = 0$) and heat generation or absorption ($\Delta = 0$) with those of Himasekhar et al. [22] and found to be in excellent agreement. This comparison is given in Table 1. In addition, the surface shear stresses and heat transfer [$-H''(0)$, $-G'(0)$, $-\theta'(0)$], and ambient velocity $-H(\infty)$ for the steady-state case in the absence of buoyancy effects ($\lambda = 0$) and with $H_0 = 0$ and $\Delta = 0$ were compared with those given by Sparrow and Cess [11] and the results were found to be in very good agreement. These comparisons are shown in Tables 2 and 3.

Fig. 2 displays representative profiles for the tangential velocity [$-H'(\eta, t^*)$] for various values of the buoyancy ratio N for both increasing and decreasing angular velocities [$\phi(t^*) = 1 + \epsilon t^{*2}$, $\epsilon = \pm 0.2$] when $H_0 = 0$, $M = 1$, $\lambda = 1$, $Pr = 0.78$, $Sc = 0.6$, $\Delta = 0$, and $t^* = 1$, respectively. It should be noted that the curve for $N < 0$ corresponds to opposing flow while those for $N > 0$ correspond to aiding flow. As expected, increases in the buoyancy ratio (or solutal buoyancy effect) cause an increase in the buoyancy-induced flow along and normal to the cone and decreases in circumferential flow and the thermal and solutal level within the boundary layer for all times. Physically speaking, as the cone rotates, the fluid near the surface of the cone is forced outward along the tangential direction due to the action of the centrifugal force. This fluid is then replaced by the fluid moving in the normal direction. Thus, there is a close relationship between the tangential and normal velocities. As the solutal buoyancy effects increase, the outflow (tangential) velocity H' increases. This causes more normal flow towards the cone resulting in an increase in the

Table 1

Comparison of heat transfer and surface shear stresses $[-\theta'(0), -G'(0), -H''(0)]$ for $t^* = M = N = H_0 = \Delta = 0$

Pr		Present results			Himasekhar et al. [22]		
		$\lambda = 0$	$\lambda = 1$	$\lambda = 10$	$\lambda = 0$	$\lambda = 1$	$\lambda = 10$
0.7	$-\theta'(0)$	0.4299	0.6121	1.0099	0.4299	0.6120	1.0097
0.7	$-G'(0)$	0.6158	0.8497	1.3992	0.6158	0.8496	1.3990
0.7	$-H''(0)$	1.0255	2.2014	8.5045	1.0256	2.2012	8.5041
2.0	$-\theta'(0)$	0.7001	0.9020	1.4477	0.7002	0.9018	1.4475
2.0	$-G'(0)$	0.6158	0.7697	1.2383	0.6158	0.7696	1.2381
2.0	$-H''(0)$	1.0255	1.9423	7.2035	1.0256	1.9421	7.2030
10	$-\theta'(0)$	1.4111	1.5663	2.3583	1.4110	1.5662	2.3580
10	$-G'(0)$	0.6158	0.6838	0.9841	0.6158	0.6837	0.9840
10	$-H''(0)$	1.0255	1.5638	5.0825	1.0256	1.5636	5.0821
100	$-\theta'(0)$	0.8522	2.9220	4.3013	2.8520	2.9218	4.3010
100	$-G'(0)$	0.6158	0.6289	0.7376	0.6158	0.6288	0.7374
100	$-H''(0)$	1.0255	1.2229	2.9488	1.0256	1.2227	2.9486

Table 2

Comparison of surface shear stresses $[-H''(0), -G'(0)]$ and ambient velocity $[-H(\infty)]$ for $t^* = H_0 = \lambda = \Delta = 0$

M	Present results			Sparrow and Cess [11]		
	$-H''(0)$	$-G'(0)$	$-H(\infty)$	$-H''(0)$	$-G'(0)$	$-H(\infty)$
0	1.0207	0.6159	0.8848	1.021	0.616	0.885
0.5	0.773	0.8488	0.4587	0.770	0.849	0.459
1	0.6194	1.0692	0.2531	0.619	1.069	0.253
2	0.4613	1.4418	0.1088	0.461	1.442	0.109
3	0.3813	1.7477	0.0617	0.381	1.748	0.0618
4	0.3308	2.0097	0.0406	0.331	2.010	0.0408

Table 3

Comparison of surface heat transfer $[-\theta'(0)]$ for $t^* = H_0 = \lambda = \Delta = 0$

Pr	Present results			Sparrow and Cess [11]		
	$M = 0.1$	$M = 1$	$M = 10$	$M = 0.1$	$M = 1$	$M = 10$
0	0.0763	0.3958	1.1337	0.0766	0.396	1.134
0.5	0.0426	0.2819	0.9558	0.0428	0.282	0.956
1	0.0282	0.1939	0.8011	0.0244	0.194	0.801
2	0.0107	0.0981	0.5712	0.0108	0.0982	0.571
3	0.00612	0.0587	0.4218	0.00614	0.0588	0.422
4	0.00406	0.0344	0.3181	0.00407	0.0395	0.318

normal velocity H . The increase in the tangential and normal velocities as N increases is followed by simultaneous decreases in the azimuthal velocity G , temperature θ and concentration C since the velocities H and H' act as a opposing mechanisms as seen from Eqs. (10)–(12). The effects of decreasing the angular velocity of the cone is seen to increase the flow velocities significantly with insignificant effect on both the temperature and concentration at $t^* = 1$. The behaviors regarding the tangential velocity are clearly shown in Fig. 2 while the trends of the normal and azimuthal velocities $[-H(\eta, t^*), G(\eta, t^*)]$, temperature $[\theta(\eta, t^*)]$ and concentration $[C(\eta, t^*)]$ were observed from other results not presented here for brevity.

Figs. 3–6 illustrate the effects of the buoyancy ratio N on the local skin friction coefficients in the tangential and azimuthal directions $(Re_x^{1/2} C_{fx}, 2^{-1} Re_x^{1/2} C_{fy})$, the local Nusselt number $(Re_x^{-1/2} Nu_x)$ and the local Sherwood number

$(Re_x^{-1/2} Sh_x)$ for increasing and decreasing angular velocities $[\phi(t^*) = 1 + \epsilon t^{*2}, \epsilon = \pm 0.2]$ when $H_0 = 0, M = 1, \lambda = 1, Pr = 0.78, Sc = 0.6, \Delta = 0, 0 \leq t^* \leq 2$, respectively. The effect of the time variation is more pronounced for large t^* ($t^* > 1$). For a fixed value of N , the local skin friction coefficients, the local Nusselt number and the local Sherwood number increase with an increasing angular velocity, but the reverse trend is predicted for a decreasing angular velocity. However, these are not a mirror reflection of each other. The skin-friction coefficients and the Nusselt and Sherwood numbers are found to be strongly dependent on N for all t^* . The skin-friction coefficients in the tangential and azimuthal directions $(Re_x^{1/2} C_{fx}, 2^{-1} Re_x^{1/2} C_{fy})$ and the Nusselt and Sherwood numbers $(Re_x^{-1/2} Nu_x, Re_x^{-1/2} Sh_x)$ increase with increasing values of N . Inspection of Fig. 2 shows clearly that the gradient of the velocity in the tangential direction and hence, the skin-friction coefficient in the tangential di-

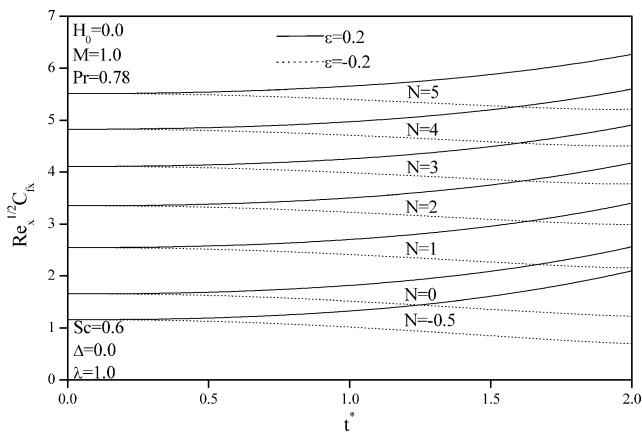


Fig. 3. Effect on N on $Re_x^{1/2} C_{fx}$.

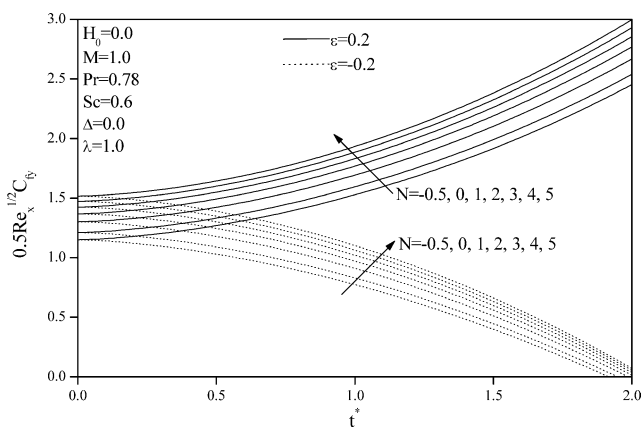


Fig. 4. Effect on N on $0.5 Re_x^{1/2} C_{fy}$.

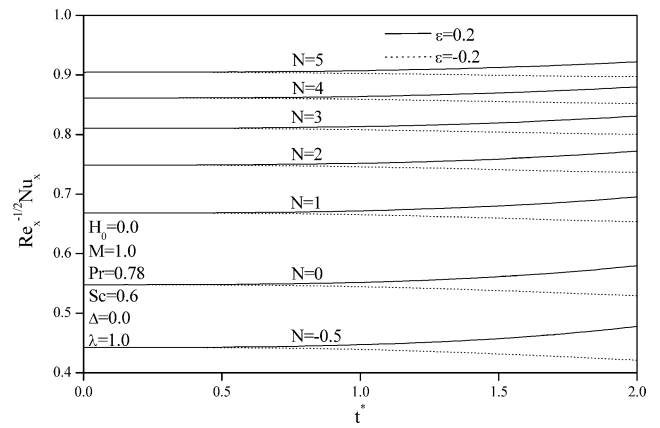


Fig. 5. Effect on N on $Re_x^{-1/2} Nu_x$.

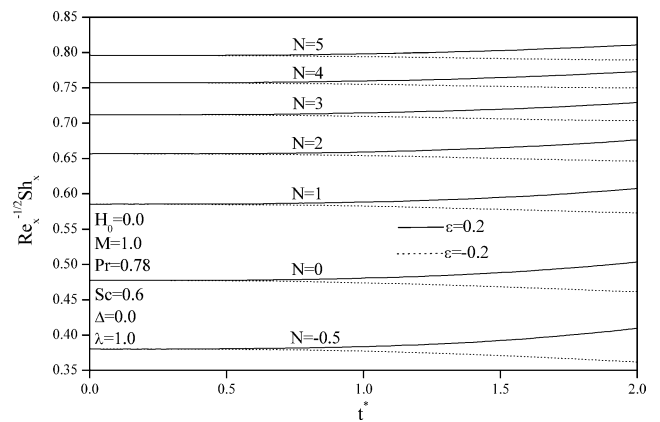


Fig. 6. Effect on N on $Re_x^{-1/2} Sh_x$.

rection increases with increasing values of N . Also, as mentioned before, all of the azimuthal velocity, temperature and concentration are reduced everywhere and their boundary layers become thinner as N increases. This causes increases in the negative wall gradients of the azimuthal velocity, temperature and concentration and, hence, in the skin-friction coefficient in the azimuthal direction, Nusselt number and Sherwood number. The effect of decreasing the angular velocity of the cone is seen to cause reductions in all of C_{fx} , C_{fy} , Nu_x and Sh_x due to the decreases in the wall gradient of H and negative wall gradients of G , θ and C . These and all previous trends are obvious from Figs. 3–6.

The effect of the suction or injection parameter H_0 on the local skin friction coefficients in the tangential and azimuthal directions ($Re_x^{1/2} C_{fx}$, $2^{-1} Re_x^{1/2} C_{fy}$) and the local Nusselt and Sherwood numbers ($Re_x^{-1/2} Nu_x$, $Re_x^{-1/2} Sh_x$) is presented in Figs. 7–10 for $\phi(t^*) = 1 + \epsilon t^{*2}$, $\epsilon = \pm 0.2$, $M = 1$, $N = 1$, $Pr = 0.78$, $Sc = 0.6$, $\lambda = 1$ and $\Delta = 0$ in the time range $0 \leq t^* \leq 2$, respectively. Imposition of fluid wall suction ($H_0 < 0$) tends to decrease the boundary layers regions causing the negative wall gradients of the azimuthal velocity, temperature and concentration to increase resulting in higher azimuthal skin-friction coefficient, Nusselt number and Sherwood number for all times. However,

the wall gradient of the tangential velocity tends to decrease yielding a net decrease in the tangential skin-friction coefficient for all times. On the other hand, injection or blowing of fluid ($H_0 > 0$) from the cone surface into the boundary layer cause the different boundary layers to stretch producing lower tangential and azimuthal skin-friction coefficients and Nusselt and Sherwood numbers for all times. As mentioned before, the effect of reducing the angular velocity of the cone results in significant reductions in C_{fx} and C_{fy} and slight reductions in Nu_x and Sh_x for times $t^* > 1$. These features are clear from Figs. 7–10.

Fig. 11 presents the effect of the heat generation or absorption coefficient Δ on the temperature profiles for both increasing and decreasing angular velocities at $t^* = 1$. Physically speaking, the presence of heat generation effects has the tendency to increase the thermal state of the fluid causing its temperature and thermal boundary layer to increase. On the other hand, when heat absorption effects are present, the reverse trends where both the fluid temperature and its thermal boundary layer decrease are produced. This is evident from Fig. 11. For a strong heat source (heat generation, $\Delta = 1.5$), it is predicted that the fluid temperature in the boundary layer region close to the cone surface becomes higher than that of the surface. This causes the temperature gradient at the surface to become positive and consequently,

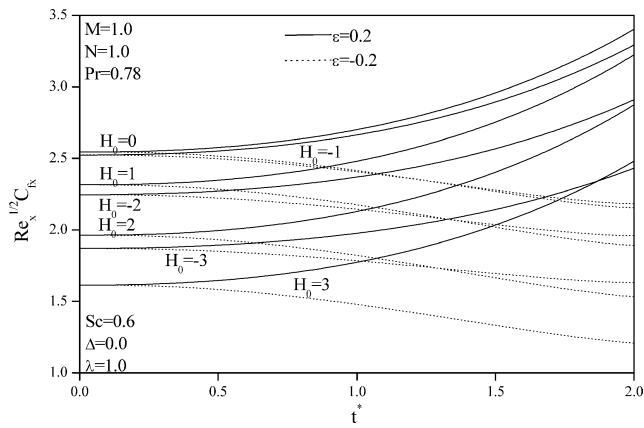


Fig. 7. Effect on H_0 on $Re_x^{1/2} C_{fx}$.

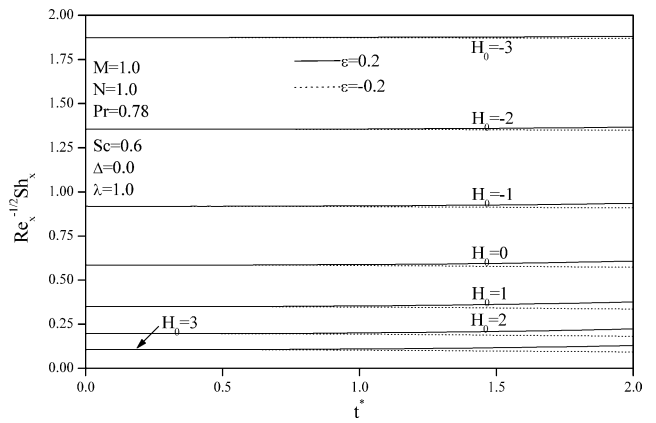


Fig. 10. Effect on H_0 on $Re_x^{-1/2} Sh_x$.

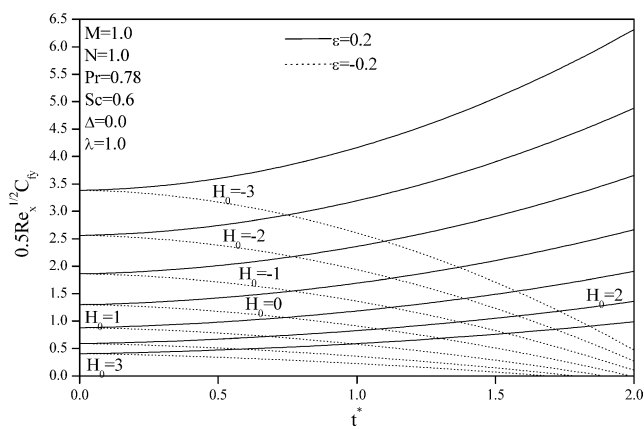


Fig. 8. Effect on H_0 on $0.5 Re_x^{1/2} C_{fy}$.

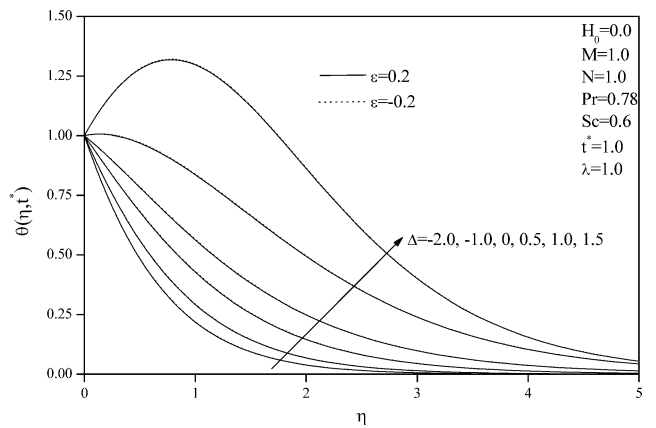


Fig. 11. Effect of Δ on temperature profiles $\theta(\eta, t^*)$.

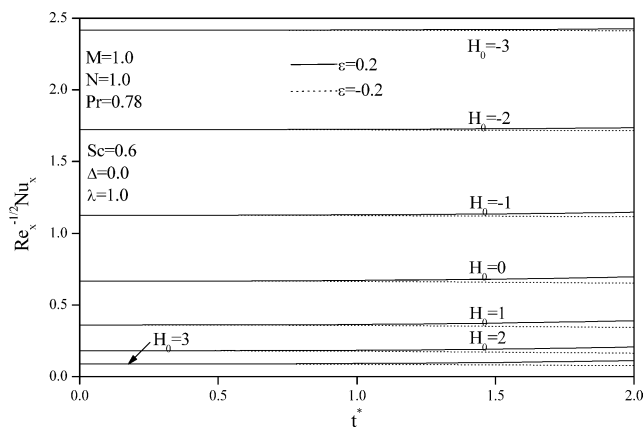


Fig. 9. Effect on H_0 on $Re_x^{-1/2} Nu_x$.

the Nusselt number at $t^* = 1$ to become negative. This will be seen in the next figures. The effect of increasing or decreasing the angular velocity on the temperature profile for a specific value of Δ is seen to be insignificant.

The effect of the heat generation or absorption coefficient Δ on the tangential skin-friction coefficient ($Re_x^{1/2} C_{fx}$) and the Nusselt and Sherwood numbers ($Re_x^{-1/2} Nu_x$, $Re_x^{-1/2} Sh_x$) for $\phi(t^*) = 1 + \epsilon t^{*2}$, $\epsilon = \pm 0.2$ in the time range $0 \leq t^* \leq 2$

is displayed in Figs. 12–14, respectively. The tangential skin-friction coefficient and the Sherwood number are predicted to increase while the Nusselt number is predicted to decrease with increases in the values of Δ . The reason for this trend in the Nusselt number is that the thermal boundary layer increases with increasing values of Δ as mentioned before. Consequently, the negative temperature gradient and hence the Nusselt number decreases with increasing values of Δ for all times. As mentioned before, the negative values in the Nusselt number are due to the fact that, for relatively large heat generation effects ($\Delta = 1$ and $\Delta = 1.5$), the fluid temperature in the boundary layer region close to the cone surface becomes higher than that of the surface. This produces a positive temperature gradient at the surface and consequently, the Nusselt number becomes negative. In addition, increases in the values of Δ produces higher temperatures, higher induced tangential flow and lower concentration levels. This causes the wall tangential velocity gradient and the negative concentration gradient at the surface to increase. This results in increases in the tangential skin-friction coefficient and Sherwood number. Furthermore, while the angular velocity is seen to affect the tangential skin-friction coefficient and the Sherwood number significantly for $t^* > 0.5$, the Nusselt number is affected only slightly for times greater than 1.5. These trends are shown in Figs. 12–14.

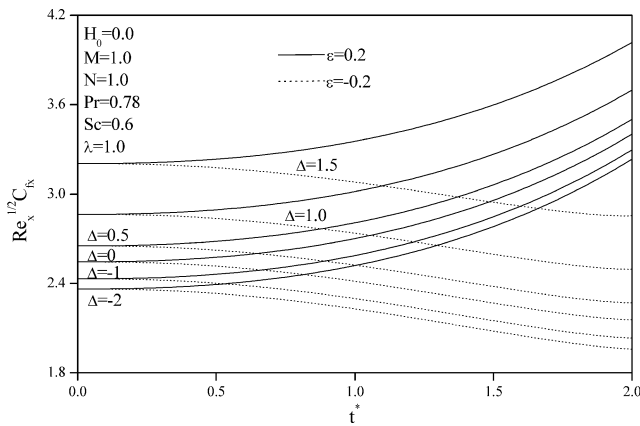


Fig. 12. Effect of Δ on $Re_x^{-1/2} C_{f,x}$.

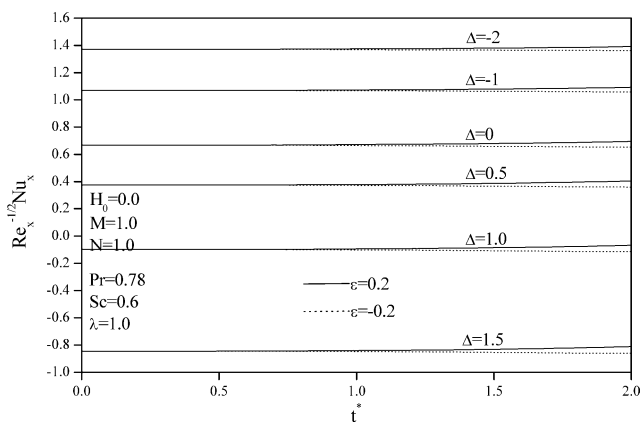


Fig. 13. Effect of Δ on $Re_x^{-1/2} Nu_x$.

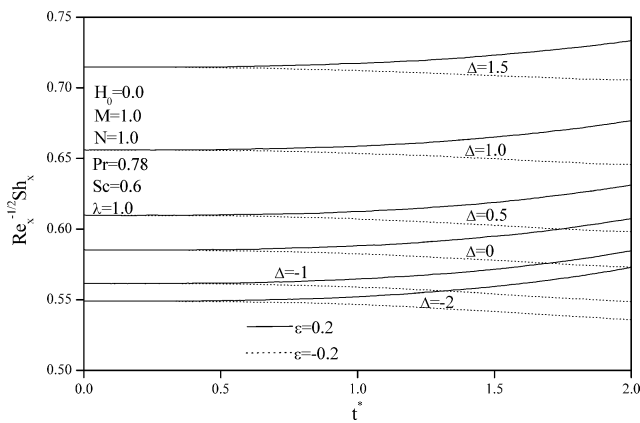


Fig. 14. Effect of Δ on $Re_x^{-1/2} Sh_x$.

5. Conclusions

The problem of unsteady heat and mass transfer by mixed convection flow over a vertical permeable cone rotating in an ambient fluid with a time-dependent angular velocity in the presence of a magnetic field and heat generation or absorption effects was studied. The cone surface was maintained at variable temperature and concentration. Fluid suction or injection was assumed to occur at the cone surface. The cou-

pled nonlinear partial differential equations governing the thermosolutal mixed convective flow were solved numerically using an implicit, iterative finite-difference scheme. Comparisons with previously published work were performed and the results were found to be in excellent agreement. It was found that the local tangential and azimuthal skin-friction coefficients and local Nusselt and Sherwood numbers increased with time when the angular velocity of the cone increased, but the reverse trend was observed for a decreasing angular velocity. However, these were not mirror reflection of each other. Increasing the buoyancy ratio was predicted to increase the skin-friction coefficients and the Nusselt and Sherwood numbers. Also, increases in the heat generation or absorption coefficient increased the local tangential skin-friction coefficient and Sherwood number and decreased the local Nusselt number. On the other hand, the azimuthal skin-friction coefficient and the Nusselt and Sherwood numbers increased with the increase in the suction parameter while the reverse effect was obtained as the injection parameter was increased.

References

- [1] H.S. Takhar, A. Chamkha, G. Nath, Unsteady mixed convection flow from a rotating vertical cone with a magnetic field, *Heat Mass Transfer* 39 (2003) 297–304.
- [2] K.C.D. Hickman, Centrifugal boiler compression still, *Indust. Engrg. Chem.* 49 (1957) 786–800.
- [3] S. Ostrach, W.H. Brown, Natural convection inside a flat rotating container, NACA TN 4323, 1958.
- [4] L.A. Dorffman, Hydrodynamic Resistance and the Heat Loss of Rotating Solids, Oliver and Boyd, Edinburgh, 1963 (Trans. by N. Kemmer).
- [5] F. Kreith, Convective heat transfer in rotating systems, in: T.V. Irvine, J.P. Hartnett (Eds.), *Advances in Heat Transfer* 5 (1968) 129–251.
- [6] E.M. Sparrow, J.L. Gregg, Heat transfer from a rotating disk to fluids of any Prandtl number, *J. Heat Transfer* 81 (1959) 249–251.
- [7] J.P. Hartnett, Heat transfer from anon-isothermal disk rotating in still air, *J. Appl. Mech* 26 (1959) 672–673.
- [8] C.L. Tien, I.J. Tsuji, A theoretical analysis of laminar forced flow and heat transfer about a rotating cone, *J. Heat Transfer* 87 (1965) 184–190.
- [9] T.C.Y. Koh, J.F. Price, Nonsimilar boundary layer heat transfer of a rotating cone in forced flow, *J. Heat Transfer* 89 (1967) 139–145.
- [10] J.P. Hartnett, E.C. Deland, The influence of Prandtl number on the heat transfer from rotating non-isothermal disks and cones, *J. Heat Transfer* 83 (1961) 95–96.
- [11] E.M. Sparrow, R.D. Cess, Magneto hydrodynamic flow and heat-transfer about a rotating disk, *J. Appl. Mech.* 29 (1962) 181–187.
- [12] M.A. Tarek, E.L. Mishkawg, A.A. Hazem, A.M. Adel, Asymptotic solution for the flow due to an infinite rotating disk in the case of small magnetic field, *Mech. Res. Comm.* 25 (1998) 271–278.
- [13] M. Lee, D.R. Jeng, K.J. Dewitt, Laminar boundary layer transfer over rotating bodies in forced flow, *J. Heat Transfer* 100 (1978) 496–502.
- [14] C.Y. Wang, Boundary layers on rotating cones, disks and axisymmetric surfaces with concentrated heat source, *Acta Mech.* 81 (1990) 245–251.
- [15] R.G. Hering, R.J. Grosh, Laminar free convection from a non-isothermal cone at low Prandtl number, *Internat. J. Heat Mass Transfer* 8 (1965) 1333–1337.
- [16] S. Roy, Free convection from a vertical cone at high Prandtl numbers, *J. Heat Transfer* 96 (1974) 115–117.

- [17] M. Alamgir, Over-all heat transfer from vertical cones in laminar free convection: an approximate method, *J. Heat Transfer* 101 (1979) 174–176.
- [18] T.Y. Na, J.P. Chiou, Laminar natural convection over a slender vertical frustum of a cone, *Warme- und Stoffubertragung* 12 (1979) 83–87.
- [19] T.Y. Na, J.P. Chiou, Laminar natural convection over a frustum of a cone, *Appl. Sci. Res.* 35 (1979) 409–421.
- [20] K.A. Yih, Effect of radiation on natural convection about a truncated cone, *Internat. J. Heat Mass Transfer* 42 (1999) 4299–4305.
- [21] R.G. Hering, R.H. Grosh, Laminar combined convection from a rotating cone, *J. Heat Transfer* 85 (1963) 29–34.
- [22] K. Himasekhar, P.K. Sarma, K. Janardhan, Laminar mixed convection from a vertical rotating cone, *Internat. Comm. Heat Mass Transfer* 16 (1989) 99–106.
- [23] D. Anilkumar, S. Roy, Unsteady mixed convection flow on a rotating cone in a rotating fluid, *Appl. Math. Comput.* 155 (2004) 545–561.
- [24] M.C. Ece, An initial boundary layer flow past a translating and spinning rotational symmetric body, *J. Engrg. Math.* 26 (1992) 415–428.
- [25] A. Ozturk, M.C. Ece, Unsteady forced convection heat transfer from a translating and spinning body, *J. Heat Transfer* 117 (1995) 318–323.
- [26] H.S. Takhar, A. Chamkha, G. Nath, Unsteady laminar MHD flow and heat transfer in the stagnation region of an impulsively spinning and translating sphere in the presence of buoyancy forces, *Heat Mass Transfer* 37 (2001) 397–402.
- [27] S. Roy, D. Anilkumar, Unsteady mixed convection from a rotating cone in a rotating fluid due to the combined effects of thermal and mass diffusion, *Internat. J. Heat Mass Transfer* 47 (2004) 1673–1684.
- [28] K.R. Cramer, S.I. Pai, *Magnetofluid Dynamics for Engineers and Applied Physicists*, Scripta Publishing Company, Washington, DC, 1973.
- [29] F.G. Blottner, Finite-difference method of solution of the boundary layer equations, *AIAA J.* 8 (1970) 193–205.